Fish and Shellfish Immunology 94 (2019) 434–446

Contents lists available at ScienceDirect

Fish and Shellfish Immunology

journal homepage: www.elsevier.com/locate/fsi

Full length article

Molecular characterization of *carboxypeptidase B-like* (CPB) in *Scylla paramamosain* and its role in white spot syndrome virus and *Vibrio alginolyticus* infection

Xiyi Qian, Yongyong Lai, Fei Zhu*

Zhejiang Provincial Engineering Laboratory for Animal Health Inspection and Internet Technology, College of Animal Science and Technology, Zhejiang Agriculture and Forestry University, Hangzhou, 311300, China

ARTICLE INFO

Keywords:
Scylla paramamosain
Carboxypeptidase B-Like
White spot syndrome virus
Vibrio alginolyticus
Apoptosis

ABSTRACT

Carboxypeptidase plays an important physiological role in the tissues and organs of animals. In this study, we cloned an entire 2316 bp *carboxypeptidase B-like (CPB)* sequence with a 1302 bp open reading frame encoding a 434 amino acid peptide from *Scylla paramamosain*. The *CPB* gene was expressed highly in hepatopancreas and decreased in crab hemocytes after challenges with white spot syndrome virus (WSSV) or *Vibrio alginolyticus*. After *CPB* gene knockdown using double-stranded RNA (CPB-dsRNA), the expression of *JAK*, *STAT*, *C-type lectin*, *crustin antimicrobial peptide*, *Toll-like receptors*, *prophenoloxidase*, and *myosin II essential light chain-like protein* were down-regulated in hemocytes at 24 h post dsRNA treatment. *CPB* knockdown decreases total hemocyte count in crabs indicated that CPB may negatively regulate crab hemocyte proliferation in crabs. CPB showed an inhibitory effect on hemocyte apoptosis in crabs infected with WSSV or *V. alginolyticus*. The phagocytosis rate of WSSV by hemocytes was increased after CPB-dsRNA treatment. After WSSV challenge, the mortality and WSSV copy number were both decreased but the rate of hemocyte apoptosis was increased in CPB-dsRNA-treated crabs. The results indicate that the antiviral activity of the crabs was enhanced when CPB was knocked down, indicating WSSV may take advantage of CPB to benefit its replication. In contrast, the absence of CPB in crabs increased mortality following the *V. alginolyticus* challenge. The phagocytosis rate of *V. alginolyticus* by hemocytes was increased after CPB-dsRNA treatment. It was revealed that CPB may play a positive role in the immune response to *V. alginolyticus* through increasing the phagocytosis rate of *V. alginolyticus*. This research further adds to our understanding of the CPB and identifies its potential role in the innate immunity of crabs.

1. Introduction

Scylla paramamosain is mainly distributed in southern China and other Asian countries. It is an important species commercially and widely cultured in China [1,3]. Because of its fast growth, large size, delicious taste, high nutritional value, and adaptability, *S. paramamosain* is one of the most important aquaculture crabs [4]. In recent decades, the rapid development of large-scale mud crab cultivation has been accompanied by the emergence of various diseases caused by bacteria, viruses, and rickettsia-like organisms, resulting in huge economic losses in the mud crab farming industry [5]. Vibriosis and white spot syndrome virus (WSSV) are two of the most serious diseases in crabs and have caused irreversible damage to the crab culture industry worldwide [6]. During WSSV infection, the virus relies on the metabolic mechanism of living cells to complete its life cycle and disrupt the normal metabolism of the host cells [7]. When the virions mature, the damage to host cell metabolism will lead to cell death, which in turn releases new virions [8–11]. Vibrio is a Gram-negative bacterium and one of the main pathogens of brackish water crabs in southeastern China. After vibrio infection, the *S. paramamosain* shows symptoms of lethargy, loss of appetite, decreased intake, and discoloration of the carapace. The appendage of the diseased crab turns pink, the legs move, and the sputum becomes edematous. At the same time, bacterial pathogens can be observed in tissues such as blood, intestines, and stomach [12–14]. It is well known that the immune response of host to virus depends on the virus-host interaction [15]. The regulation of gene expression plays an important role in viral–host interaction. In the study of human diseases, it has been found that the expression level of the *carboxypeptidase B* (CPB) gene is related to several human diseases [16]. In addition to traditional C-terminal sequencing, protein or peptide modification and food processing, carboxypeptidase activity has been gradually recognized and applied in the diagnosis and treatment

* Corresponding author.
E-mail addresses: zhufei@zju.edu.cn, 20110050@zafu.edu.cn (F. Zhu).

https://doi.org/10.1016/j.fsi.2019.09.036
Received 5 July 2019; Received in revised form 5 September 2019; Accepted 14 September 2019
Available online 16 September 2019

of diseases [17]. However, CPB genes in invertebrates, such as *S. paramamosain*, have not been studied. In this study, we have identified a CPB in the *S. paramamosain* and studied its role in the immune process of *S. paramamosain*.

Carboxypeptidase is a specific class of peptide exonuclease that degrades and releases free amino acids one by one from the C-terminus of the peptide chain. Carboxypeptidase plays many important functions in different tissues and organs. In the digestion of food to the synthesis of neuroendocrine peptides, the function of carboxypeptidase is indispensable [18]. Carboxypeptidases are divided into two sub-categories according to substrate preference: carboxypeptidase A (cleaving aliphatic residues) and CPB (cleaving basic amino residues). In this study we have focused on CPB, it is a digestive enzyme that hydrolysates C-terminal Arginine and Lysine and was first found in the pancreas of cattle and pigs [19]. Since Arg and Lys are basic amino acids, CPB was originally named alkaline carboxypeptidase. CPB hydrolyzes the Arg of the C-terminus of protamine, and CPB can be further distinguished as plasma CPB or tissue CPB [20]. Plasma CPB is produced by the liver and circulates in plasma as an inactive precursor. The glycosylation of the plasma CPB pro-peptide distinguish it from other carboxypeptidases and stabilizes and prolongs the half-life of CPB in plasma [21]. Carboxypeptidase is inextricably linked to the development of various diseases. The expression and distribution of CPB in the brains of patients with Alzheimer's disease and healthy subjects were compared, and it was found that CPB can eliminate the accumulation and toxicity of β-starch in brain cells and protect neurons [22]. Plasma CPB can be used for tumor antibody-directed enzyme prodrug therapy and is associated with chronic liver disease, its concentrations can be used to diagnose and assess the extent of acute pancreatitis [23,24]. Since the discovery of carboxypeptidase proteins, the main functions of this conserved family have been thoroughly studied to determine their role in disease diagnosis and treatment. However, few studies have investigated the link between this essential protein and disease infections (WSSV or Vibriosis) in invertebrates.

In this project, we identified a novel CPB in *S. paramamosain* and investigated its role in virus or vibrio infection.

2. Methods and materials

2.1. Crabs and tissue preparation

The healthy adult *S. paramamosain* (approximately 100 g) were obtained from a seafood market of Hangzhou. All animal experiments were reviewed and approved by the Institutional Animal Care and Use Committee of Zhejiang A & F University (Hangzhou, China). The muscles, hepatopancreas, gills, intestines, heart and hemocytes were collected from health or challenged crabs. The samples were used immediately for RNA extraction, in order to prevent total RNA degradation. WSSV (GenBank accession no. AF332093.1) was purified and used in challenge experiments, as described previously [25]. *V. alginolyticus* was cultured and used to challenge the crabs according to the previous report [26].

2.2. Rapid amplification of cDNA ends (RACE)

Total RNA was extracted from hepatopancreas of the *S. paramamosain* using RNApure Tissue & Cell Kit (CWBIO, China), following the protocol of the manufacturer. The concentration and quality of total RNA were determined by the Nanodrop Trac Spectrophotometer and 1% agarose gel electrophoresis detection, respectively. The RACE technique was utilized to clone the full-length cDNA sequence of the gene, based on the known middle fragment using SMARTer® RACE 5′/3′Kit, following the protocol of the manufacturer. The synthesized cDNA were kept at −20 °C, used for the 3′/5′ -RACE PCR with 3′ gene-specific primer (3GSP, 3NGSP) or 5′ GSP (5GSP, 5NGSP), designed on the basis of middle sequence (the primer's sequences are shown in Table 1). The PCR products were purified using MiniBEST Agarose Gel DNA Extraction Kit Ver. 4.0 (Takara, Japan), following the manufacturer's instruction. Amplified cDNA fragments were transferred into the pMD19-T vector (Takara, Japan). Recombinant bacteria were identified by blue/white screening and confirmed by PCR and sent to sequencing company (SunYa, China). Nucleotide sequences of the cloned cDNA were sequenced by double pass. All primers used in this experiment were designed using Primer Premier 5.0.

Table 1
Universal and specific primers used in this study.

Name	Nucleotide Sequence (5′–3′)	purpose
F	AGGCCGGGTTAGACCATAG	for the conservative fragment
R	AGTAGCCAGAATGACGCAAT	for the conservative fragment
3'race GSP	CCACAGACGACTGGGCTTACGGAG	for 3′RACE
3'race NGSP	GCGAACTATCGTGGCGGGTGTGTT	for 3′RACE
5'race GSP	AAGTGGTGACAGCGGGTGAGAT	for 5′RACE
5'race NGSP	TCCAGTCCATCGGGAAGTTAGT	for 5′RACE
CPB-dsRNA-F	AAGCTTAGGCCGGGTTAGACCATAG	for CPB RNAi
CPB-dsRNA-R	GAATTCCGTTGACTCGTCGGTTCTT	for CPB RNAi
CPB-real time-F	GACATTTCGTAGACCATCACC	for CPB expression
CPB-real time-R	GAACTTGCCACTATACAGCGT	for CPB expression
GAPDH-real time-F	ACCTCACCAACTCCAACAC	for GAPDH expression
GAPDH-real time-R	CATTCACAGCCACAACCT	for GAPDH expression
C-type-lectin-F	ACTGAGGGGAAAGTAGCC	for C-type-lectin expression
C-type-lectin-R	TGCCCGTGTTTATTCATC	for C-type-lectin expression
crustin-F	TCAGAGCACCCTGGTAAATGT	for crustin antimicrobial
crustin-R	GGCAGAACTGCGAAAGAAAG	for crustin antimicrobial
JAK-F	ATTGCTGAGGGGATGGATT	for JAK expression
JAK-R	GCCCATCACATTCCCAAA	for JAK expression
proPO-F	ATGAAAGAGGAGTGGAGATG	for prophenoloxidase expression
proPO-R	GTGATGGATGAGGAGGTG	for prophenoloxidase expression
TLR-F	TGTTGCCAGAGCAGAAGGT	for toll-like receptor expression
TLR-R	TTCCGTGAATGAACGAAGG	for toll-like receptor expression
myosin-F	GCCGAGATAAGTGTAGAGGAA	for myosin II essential-light-chain-like-protein expression
myosin-R	AGTGGGGTTCTGTCCAAG	for myosin II essential-light-chain-like-protein expression
STAT-F	GACTTCACTAACTTCAGCCTCG	for STAT expression
STAT-R	GAGCTGAGTCTGTCTTAATGTTATCC	for STAT expression

2.3. Nucleotide sequence and bioinformatics analyses

The nucleotide sequence similarities were examined by BLAST software (http://www.ncbi.nlm.nih.gov/BLAST/). The 5′and 3′sequences from RACEs were assembled with the partial cDNA sequences corresponding to each fragmental sequence by DNAMAN 5.0. The protein prediction was performed using the open reading frame (ORF) Finder tool. Multiple sequence alignment was created by using the Clustal 1.81. And the phylogenetic trees based on the amino acid sequences were performed by the neighborjoining method using Molecular Evolutionary Genetics Analysis, MEGA 7.1.

2.4. The quantitative real-time PCR

Relative CPB mRNA expression levels in various adult tissues were measured by qRT-PCR using a SYBR II® Premix Ex Taq (Tli Rnase Plus)

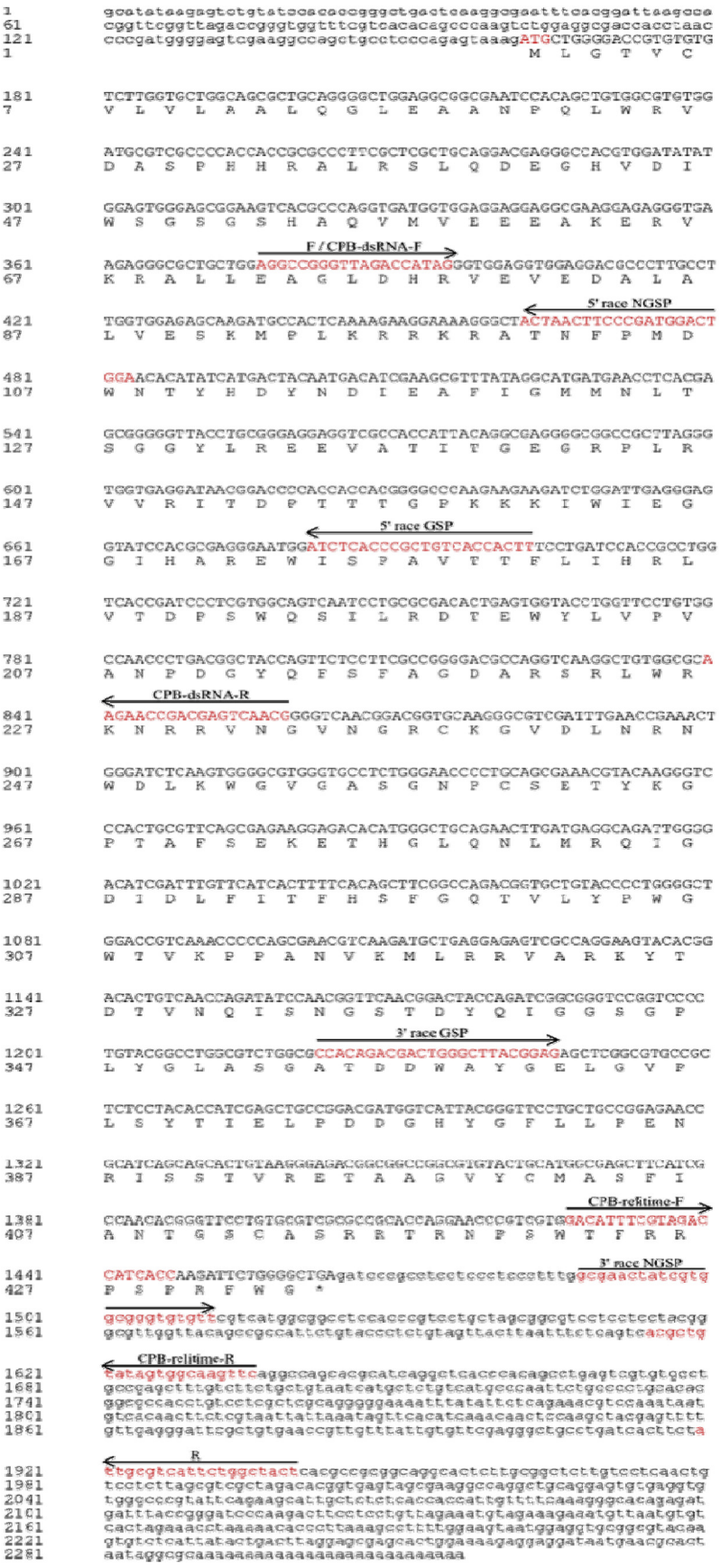

Fig. 1. Nucleotide and deduced amino acid sequence of *carboxypeptidase B-like*. The nucleotide sequence is displayed in the 5′-3'directions and numbered at the left. The deduced amino acid sequence is shown in a single capital letter amino acid code. 3′UTR and 5′UTR are shown with lowercase letters. Codons are numbered at the left with the methionine (ATG) initiation codon, an asterisk denotes the termination codon (TAG). Cloning the conservative fragment (F & R), RACE, qRT-PCR, and dsRNA primers are marked with arrows.

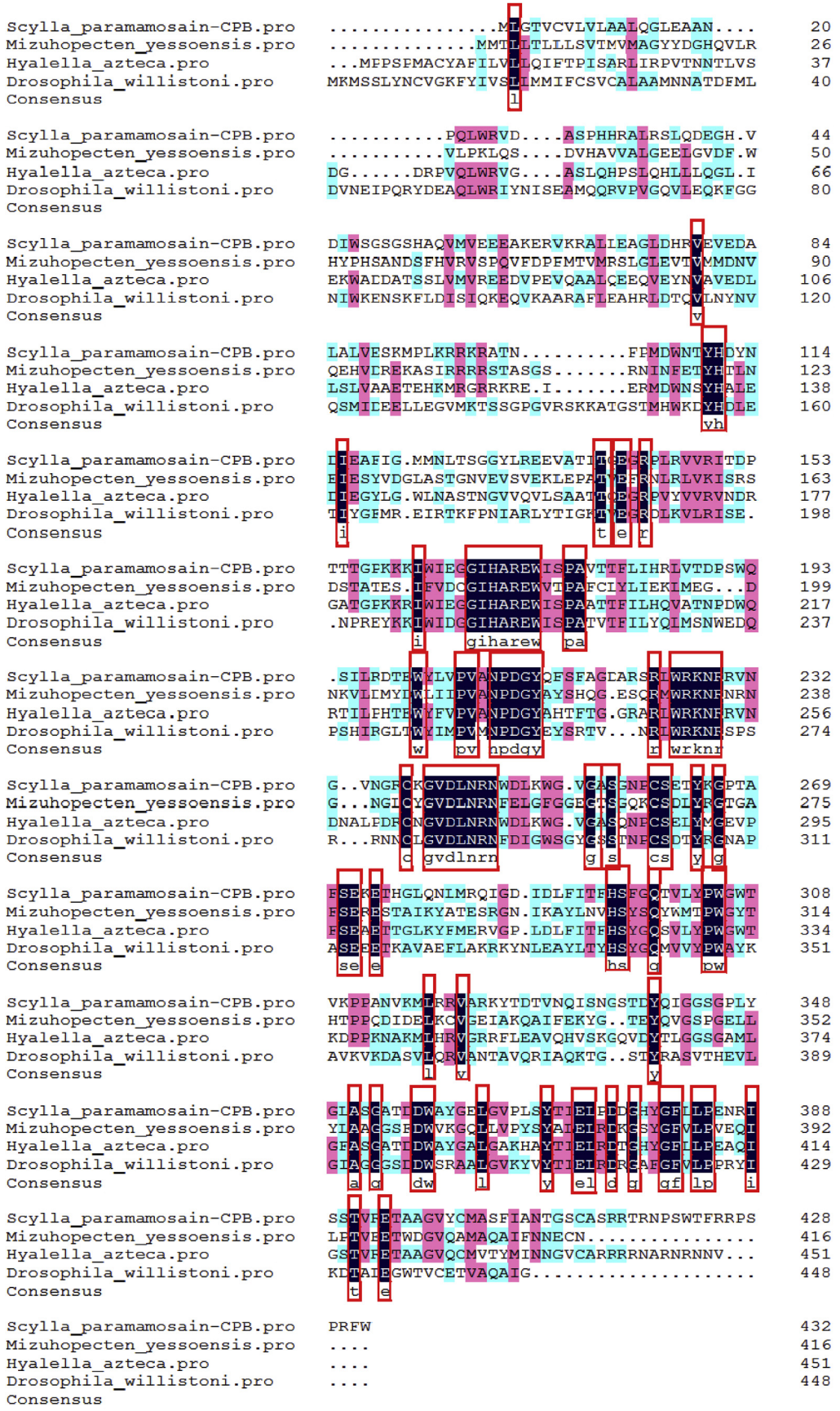

Fig. 2. Multiple alignments of amino acid sequence of *Scylla paramamosain carboxypeptidase B-like* with other *carboxypeptidase B-like* sequences of common animals. *Scylla paramamosain* (in this study), *Hyalella Azteca* (XP_018024120.1), *Mizuhopecten yessoensis* (XP_021372078.1), *Drosophila willistoni* (XP_023034853.1). Seventy-four conserved amino acids are shaded and boxed.

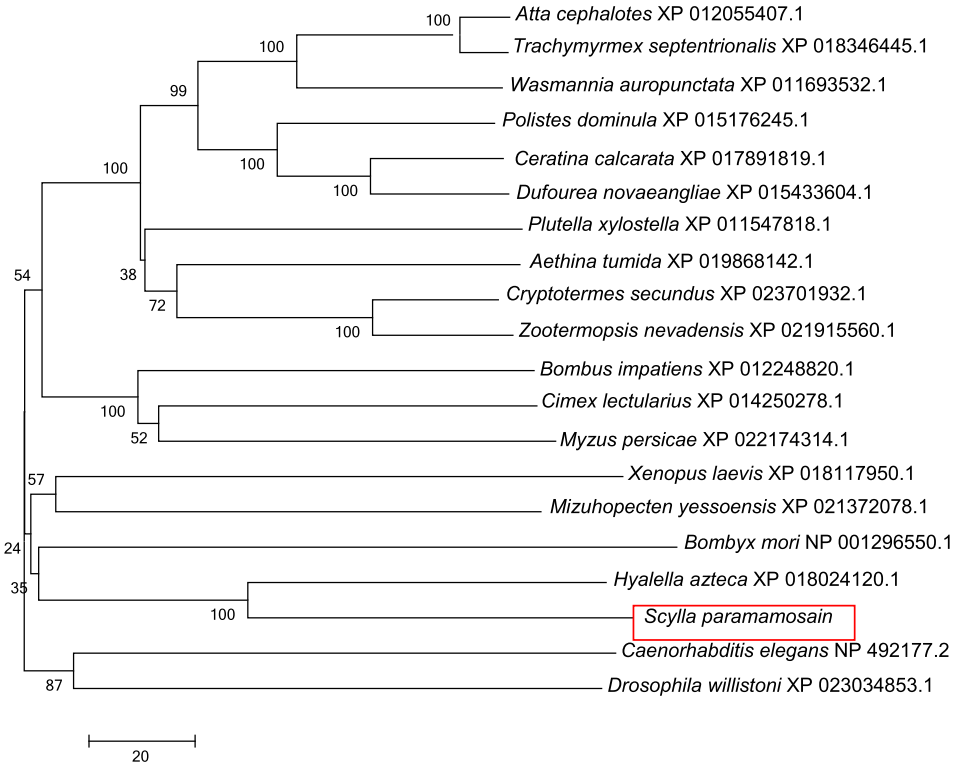

Fig. 3. The phylogenetic tree of *carboxypeptidase B-like* from different organisms based on amino acid sequence comparisons.

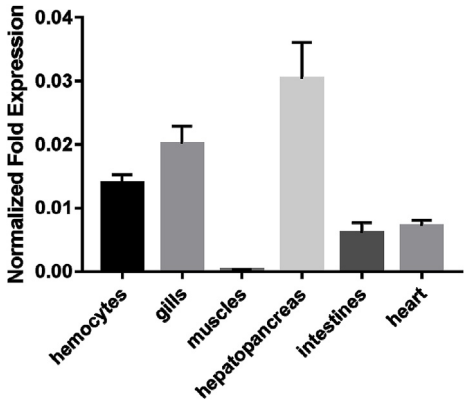

Fig. 4. Expression characterization of *carboxypeptidase B-like* in various tissues from healthy crabs revealed by qRT-PCR. The amount of *carboxypeptidase B-like* mRNA was normalized to the *GAPDH* transcript level. Data are shown as means ± standard deviation of the tissues of three separate individuals. Capital letters indicate expression of *carboxypeptidase B-like* in different adult tissues.

(Takara, Japan). Total RNA was isolated from various tissues of healthy adult crabs and hemocytes of crabs challenged by intramuscular injection of 0.1 mL of viral or bacterial suspension including WSSV (10^5 copies/mL) or *V. alginolyticus* (10^5 colony-forming units [CFU]/mL), respectively, for different times, using the RNApure Tissue & Cell Kit (CWBIO, China) according to the manufacturer's instructions. Experiments were performed in triplicate and at least three crabs were analyzed for each tissue type. The cDNA synthesis was carried out using 200 μg of total RNA with the ReverTra Ace qPCR RT Master Mix with gDNA Remover (Code: FSQ-301; Toyobo, Japan). The qRT-PCR was performed in a total volume of 10 μl containing 5 μl of SYBR® Premix Ex Taq, 0.2 μl of 10 μM forward and reverse primers, and 100 ng of cDNA template. The qRT-PCR was carried out in Bio-Rad Two Color Real-Time PCR Detection System and the data were calculated according to the $2^{-\Delta\Delta CT}$ comparative CT method by Office Excel, with the glyceraldehyde 3-phosphate dehydrogenase (GAPDH) amplification as the internal control [27]. The design and synthesis of the qRT-PCR primers were entrusted to Shanghai Generay Bio. Co., Ltd (China), based on the open reading frame (ORF). The primer sequences are shown in Table 1. The PCR conditions were 95 °C for 1 min, followed by 40 cycles at 95 °C for 15 s and 60 °C for 45 s.

2.5. Prokaryotic expression and purification of CPB-dsRNA

The primers (shown in Table 1) with specific restriction sites (Hind III in the forward primer and EcoR I in the reverse primer) were designed from the cloned nucleotide sequence. PCR product digested with Hind III/EcoR I was subcloned into LITMUS 38i Vector (NEB, MA, USA) digested with the same enzymes to gain plasmid L38i-CPB. The constructed L38i-CPB was verified by restriction enzyme digestion and DNA sequencing. The recombinant plasmid L38i-CPB was transformed into HT115 (DE3) cells. Single colonies of the above engineering bacteria were separately inoculated to 5 ml of LB medium containing Amp (100 mg/mL), cultured at 37 °C with shaking at 200 rpm for 12–16 h, and then inoculated to LB medium containing Amp by proportion of 1%, cultured at 37 °C with shaking at 200 rpm for 2–3 h (OD600 ≈ 0.6), and added with IPTG (with a final concentration of 0.8 mmol/L) to induce the expression for 4 h. After purifying with mirVana miRNA™ Isolation Kit (Ambion, USA), the xx-dsRNAs were annealed and precipitated with 5 M sodium acetate and anhydrous alcohol.

2.6. Knock down of carboxypeptidase B-like by RNAi and challenge experiments

Total RNA was purified using the RNApure Tissue & Cell Kit (CWBIO, China), following the manufacturer's instructions. CPB-dsRNAs (75 μg/crab) was immediately injected intramuscularly into crabs, and carboxypeptidase B-like mRNA expression levels were detected by qRT-PCR following WSSV and *V. alginolyticus* challenge. Crabs were divided into four groups: intramuscular injection with 100 μL PBS

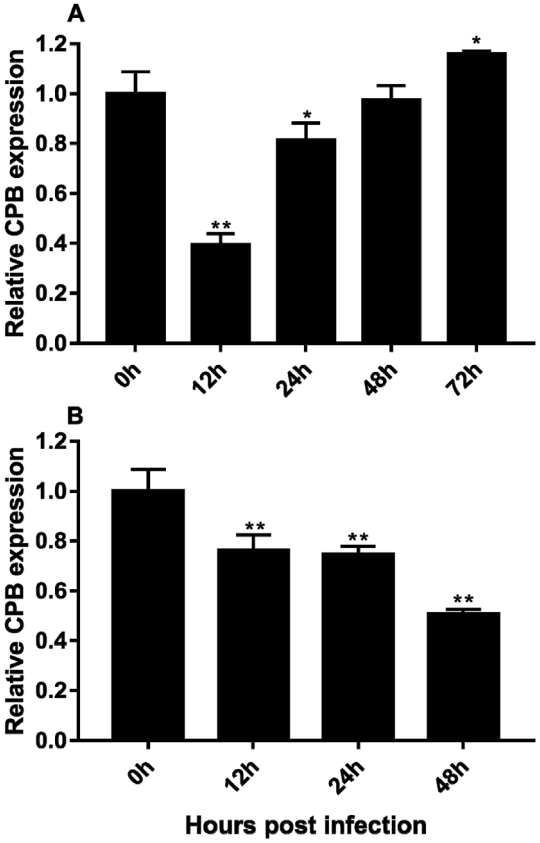

Fig. 5. qRT-PCR analysis of *carboxypeptidase B-like* expression challenged with WSSV or *V. alginolyticus*. (A) qRT-PCR analysis of *carboxypeptidase B-like* expression in the hemocytes of *S. paramamosain* challenged with WSSV. (B) qRT-PCR analysis of *carboxypeptidase B-like* expression in the hemocytes of *S. paramamosain* challenged with *V. alginolyticus*. The amount of *carboxypeptidase B-like* mRNA was normalized to the *GAPDH* transcript level. Data are shown as means ± SD (standard deviation) of three separate individuals in the tissues. Double asterisks indicate a significant difference (**$p < 0.01$) between two samples.

alone; intramuscular injection with CPB-dsRNA, 75 μg/crab alone; injection with CPB-dsRNA for 24 h, followed by 100 μL WSSV (10^5/mL) challenge; and injection with CPB-dsRNA for 24 h, followed by 100 μL V. *alginolyticus* (10^5 CFU/mL) challenge. Crabs mortality was monitored every 12 h after the last injection.

2.7. Quantitative analysis of WSSV

TaqMan real-time PCR was performed by using a Perfect Real Time premix (Takara, Japan) containing a high-performance Taq antibody, Takara Ex Taq HS, for hot start real-time PCR. Primers were designed using Primer 5.0 software and the TaqMan probe with the WSSV whole sequence. WSSV specific primers (5′-TTGGTTTCATGCCCGAGATT-3′) and (5′- CCTTGGTCAGCCCCTTGA-3′) produced a fragment of 57 bp after amplification. The TaqMan probe was synthesized and labeled with the fluorescent dyes 5-carboxyfluorescein (FAM) (5′-FAM-TGCTG CCGTCTCCAA-TAMRA-3′). The PCR mixture (10 μl) consisted of 5 μl Perfect Real Time premix, 200 ng DNA template, 0.2 μl of 10 μM primers, and 0.2 μl of 10 μM TaqMan fluorogenic probe at a final concentration of 0.2 μM. The DNA template was extracted from the crab hemocytes using a cell/tissue genomic DNA extraction kit (Generay, Shanghai, China) according to the manufacturer's instructions. Standard curve was made based on previous experiment [28]. PCR amplification was performed for 4 min at 50 °C, followed by 45 cycles of 45 s at 95 °C, 45 s at 52 °C and 45 s at 72 °C. Thermal cycling was performed on an iCycle IQ5 real-time PCR detection system (Bio-RAD, USA).

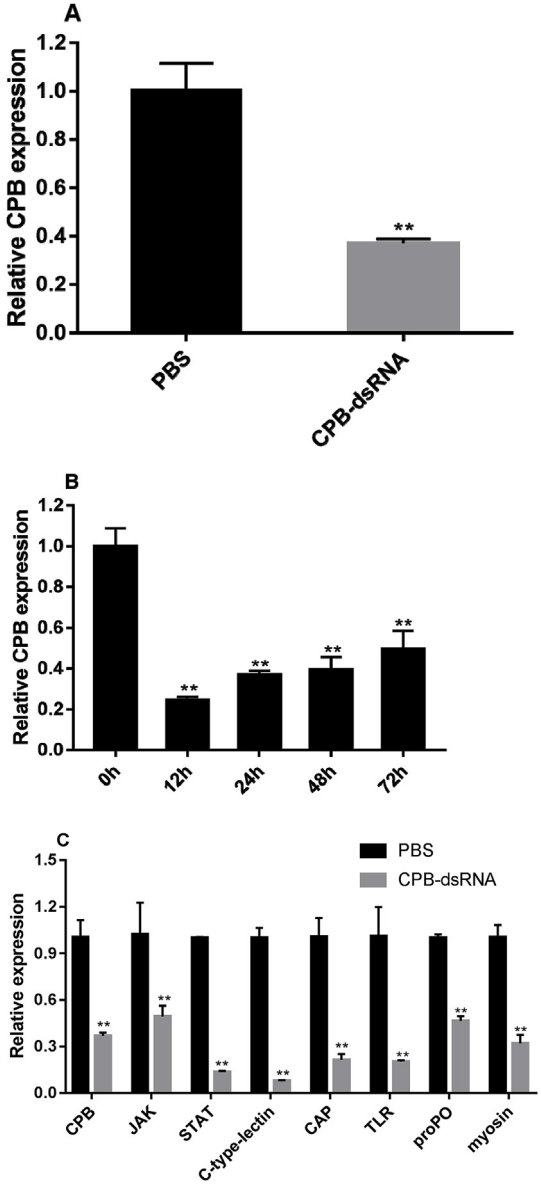

Fig. 6. qRT-PCR analysis of *carboxypeptidase B-like* and immune gene expression. (Fig. 7A) qRT-PCR analysis of *carboxypeptidase B-like* expression in the hemocytes of *S. paramamosain* treated with *carboxypeptidase B-like* dsRNA (CPB-dsRNA) at 24 h post-treatment. The amount of *carboxypeptidase B-like* mRNA was normalized to the *GAPDH* transcript level. (Fig. 7B) qRT-PCR analysis of *carboxypeptidase B-like* expression of hemocytes of *S. paramamosain* treated with CPB-dsRNA at different times post-treatment. (Fig. 7C) qRT-PCR analysis of seven immune genes [*crustin antimicrobial peptide (CAP)*, *C-type-lectin (CTL)*, *JAK*, *prophenoloxidase (proPO)*, *toll-like receptor (TLR)*, *myosin II essential-light-chain-like protein (myosin)* and *STAT*] expression in the hemocytes of *S. paramamosain* treated with CPB-dsRNA. The amount of *carboxypeptidase B-like* mRNA was normalized to the GAPDH transcript level. Data are shown as means ± standard deviation of tissues in three separate individuals. Double asterisks indicate a significant difference between two samples (**$p < 0.01$).

2.8. Kaplan-Meier survival analysis

For the pathogen challenge, healthy crabs were randomly distributed into eight groups (n = 10 per group, three repeat). The control group received injections of PBS alone, the CPB-dsRNA group received injections of CPB-dsRNA alone, the WSSV group received injections of

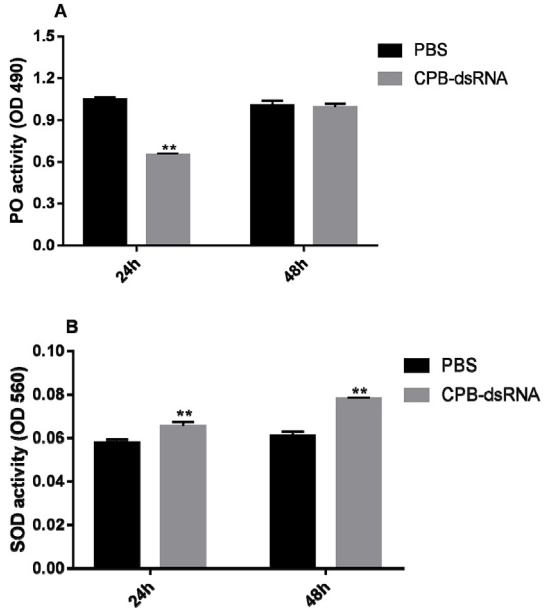

Fig. 7. PO and SOD activity of the crab treated with CPB-dsRNA. (A) PO activity of the crab treated with *carboxypeptidase B-like* dsRNA (CPB-dsRNA). (B) SOD activity of the crab treated with CPB-dsRNA. Data are expressed as percentage of control. Double asterisks indicate a significant difference (**$p < 0.01$) between the sample and the control.

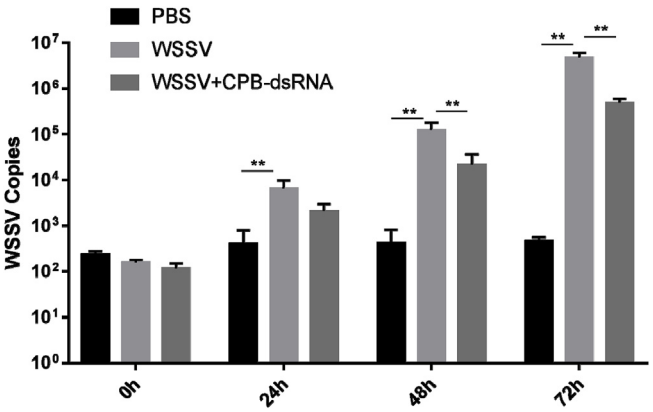

Fig. 8. Detection of WSSV copies in gills at different time (0 h, 24 h, 48 h and 72 h) post WSSV infection. The significant differences between treatments are indicated with asterisks (*$p < 0.05$; **$p < 0.01$).

WSSV in PBS, and the CPB-dsRNA + WSSV group received injections of CPB-dsRNA and WSSV, the *V. alginolyticus* group received injections of *V. alginolyticus* in PBS, and the CPB-dsRNA + *V. alginolyticus* group received injections CPB-dsRNA and *V. alginolyticus*. Each group of crabs was cultivated under the same condition. After every 12 h, the number of alive and dead crab was counted. The survival data were arranged and analyzed in Microsoft GraphPad 7.0.

2.9. Phagocyte rate counting by flow cytometry

Experimental and control groups were injected with dsRNA and PBS, respectively. In brief, 2.5 mL syringe was used to collect the hemolymph from the last walking legs of crabs which sterilized with 70% alcohol. The hemolymph was mix with the precooled anticoagulant solution (ACD-B solution: 4.8 g/L Citric Acid, 13.2 g/L sodium citrate, 14.7 g/L glucose, 1.2 g/L NaCl, pH 4.6) at ratio of 1:1, and the mixture was centrifuged at 2000 rpm at 4 °C for 10 min to collect hemolymph cells. The subsequent experiment was performed as described previously [29].

2.10. Apoptosis of crab hemocytes

The hemolymph was mixed with the precooled anticoagulant solution, ACD-B solution, at ratio of 1:1, and the mixture was centrifuged at 2000 rpm at 4 °C for 10 min to collect hemolymph cells. The hemolymph cells were then suspended in highly alkaline PBS, counted and adjusted to a density of 3–5 × 10^6 cells/mL with PBS. The cells were stained using a BD Phrmingen™ FITC Annexin V Apoptosis Kit, and assessed by flow cytometry. The cell numbers on quadrant 4, with low PI and high annexin V staining, were considered as apoptotic. The data were presented as means ± standard deviation (SD) derived from at least three independent experiments.

2.11. Determination of immune parameters after RNAi

The immune parameters determined included THC, PO and SOD activities. THC was determined as described previously. To determine total hemocyte count, hemolymph (100 μL) was withdrawn from the ventral sinus of individual crab into a 1 ml syringe containing 100 μL of 10% Methanal in 0.45 M NaCl and transferred to a microfuge tube. The hemocyte count was performed using a hemocytometer and defined as number of cells ml^{-1}, and the data presented as the total hemocyte count [30]. To determine PO and SOD activities, 500 μL hemolymph was withdrawn into a 1 mL syringe containing 500 μL ACD-B solution from each individual crab. PO activity was quantified in the hemolymph mixture based on the formation of dopa chrome from the substrate L-3, 4-dihydroxyphenylalanine (L-DOPA), as described previously [31]. SOD activity was quantified in hemocytes isolated from 300 μL of the hemolymph mixture, according to the improved method described by Beauchamp and Fridovich [32]. Data were presented as measurements.

2.12. Statistical analysis

Quantitative data were expressed as mean ± standard deviation (SD). Data from three independent experiments were analyzed by one-way analysis of variance to calculate the means and standard deviations of the triplicate assays. Statistical differences were estimated using one-way ANOVA followed by least-significant differences (LSD) and Duncan's multiple range. The differences between the different treatments were analyzed by multiple *t*-test method. All statistics were measured using SPSS software version 19 (IBM, USA). A probability level of 0.01 was used to indicate statistical significance ($p < 0.01$).

3. Results

3.1. Characterization of carboxypeptidase B-like cDNA

The full-length *CPB* cDNA sequence was 2316 base pairs (bp) (Fig. 1) and included a 1302 bp open reading frame (ORF) encoding a 434 amino acid protein. The 5′and 3′ untranslated regions (UTRs) comprised 161 bp and 853 bp, respectively. The clone also included a poly (A) tail. The *CPB* had an estimated molecular mass of 48.514 kDa and a theoretical PI of 8.494. The nucleotide and deduced amino acid sequences of the full-length cDNA are shown in Fig. 1.

3.2. Sequence homology and phylogenetic analysis

We compared the current deduced amino acid sequence with previously reported *CPB* sequences. The ORF of the *CPB* displayed 50% identity with that of *Hyalella Azteca* (XP_018024120.1), 32.43% identity with a *CPB* in *Mizuhopecten yessoensis* (XP_021372078.1), and 29.05% identity with an enolase in *Drosophila willistoni* (XP_023034853.1) (Fig. 2). A condensed phylogenetic tree based on the

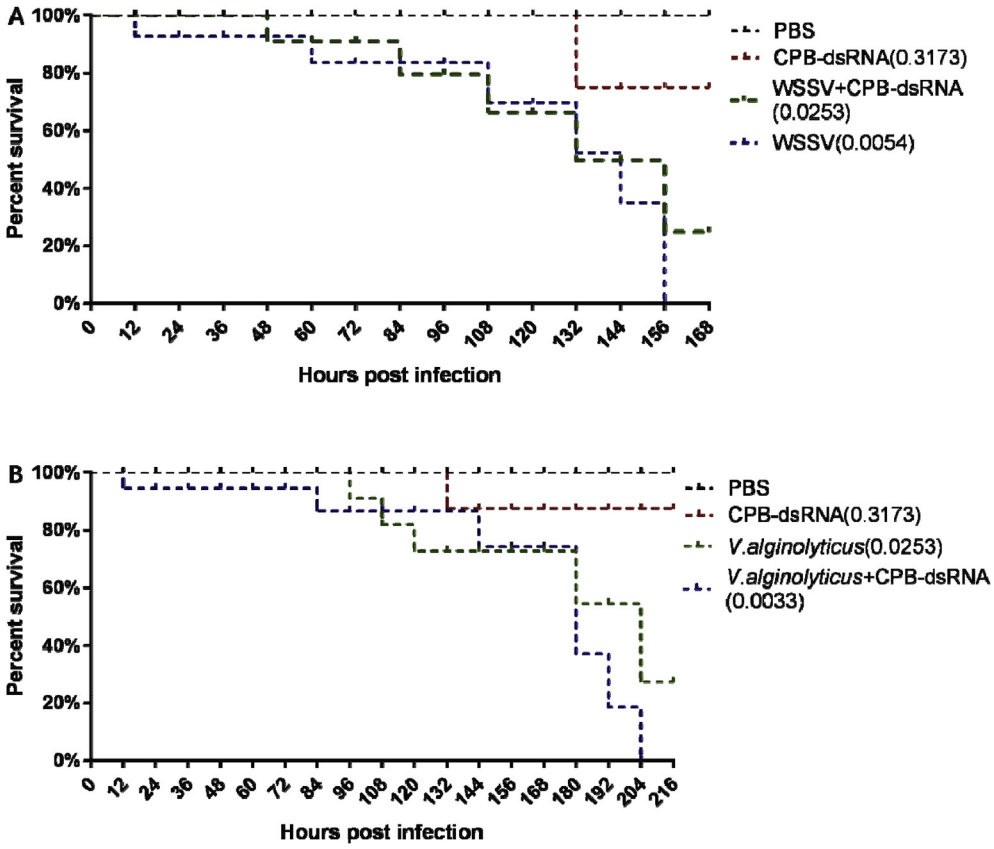

Fig. 9. The survival analysis of challenged crabs treated with CPB-dsRNA. (A) The survival analysis up from Kaplan-Meier of WSSV challenged crab treated with *carboxypeptidase B-like* dsRNA (CPB-dsRNA). (B) The survival analysis up from Kaplan-Meier of *V. alginolyticus* challenged crabs treated with CPB-dsRNA. The solutions used for injection were shown on the left. Every group has 20 individuals, respectively.

deduced amino acid sequences was constructed by the neighbor-joining method using MEGA7.1 (Fig. 3). Phylogenetic analysis showed that the *CPB* sequence was conserved among different species. The amino acid sequence revealed that conserved domains contained several highly conserved amino acid sites. Among the known species, the *S. paramamosain CPB* showed the closest relationship with that of *Hyalella Azteca*.

3.3. Tissue distribution of carboxypeptidase B-like mRNA

Expression profiling of the *CPB* gene in different tissues of *S. paramamosain* was examined by quantitative real-time polymerase chain reaction (qRT-PCR) (Fig. 4). It was significantly more highly expressed in hepatopancreas compared with other tissues and showed the lowest expression in muscle tissue. Expression levels of *CPB* in hepatopancreas were 2.17-, 1.51-, 138.43-, 5.00- and 4.25-fold greater than that in the hemocytes, gills, muscles, intestines, and heart, respectively. The expression of *CPB* in hepatopancreas was significantly higher ($p < 0.01$) than in any of the other tissues tested.

3.4. Time course of carboxypeptidase B-like expression after WSSV or V. alginolyticus challenge

We investigated the changes of *CPB* expression in crabs after challenges with WSSV or *V. alginolyticus*. *CPB* expression was significantly down-regulated ($p < 0.05$) at 12 and 24 h post-infection with WSSV, but significantly higher than the control levels at 72 h post-challenge (Fig. 5A). *CPB* expression was also significantly down-regulated ($p < 0.01$) from 12 to 48 h post-challenge with *V. alginolyticus*, with the lowest expression levels at 48 h (Fig. 5B). These results suggested that CPB may play an important role in crab innate immunity following infection with WSSV or *V. alginolyticus*.

3.5. Effects of carboxypeptidase B-like double-stranded RNA on expression of immune genes

We tested the effect of CPB double-stranded RNA (CPB-dsRNA) on mRNA expression using qRT-PCR. CPB mRNA expression in crab hemocytes was significantly knocked down by CPB-dsRNA ($p < 0.01$) (Fig. 6A). We also detected the effect of CPB-dsRNA on CPB gene expression in hemocytes of *S. paramamosain* at different time post-treatment using qRT-PCR. CPB-dsRNA inhibited the expression of CPB mRNA in hemocytes from 12 to 72 h post-treatment (Fig. 6B). We also examined the relationship between CPB expression and the expression of other immunity-related genes by analyzing the effects of CPB-dsRNA on the expression levels of important immune genes in the hemocytes of crabs. Among the seven immune genes tested, *JAK*, *STAT*, *C-type-lectin*, *crustin antimicrobial peptide (CAP)*, *Toll-like receptors (TLRs)*, *prophenoloxidase (proPO)* and *myosin II essential light chain-like protein (myosin)* were significantly down-regulated ($p < 0.01$) following treatment with CPB-dsRNA (Fig. 6C).

3.6. Determination of immune parameters

Phenoloxidase (PO) activity was significantly decreased ($p < 0.01$) in crabs treated with CPB-dsRNA at 24 h (0.6498 U), compared with the control group (1.047 U), but there was no significant difference in PO activity at 48 h (Fig. 7A). Superoxide dismutase (SOD) activity was significantly increased ($p < 0.01$) in crabs treated with CPB-dsRNA for 24 (0.0654 U) and 48 h (0.0783), compared with the controls (0.058 U and 0.061 U of control at 24 h and 48 h, respectively) (Fig. 7B). These results indicated that CPB had a stimulatory effect on the immune system in crabs.

3.7. Effects of CPB-dsRNA on WSSV copies and survival of challenged crab

Copies of WSSV increased with the duration of infection in all

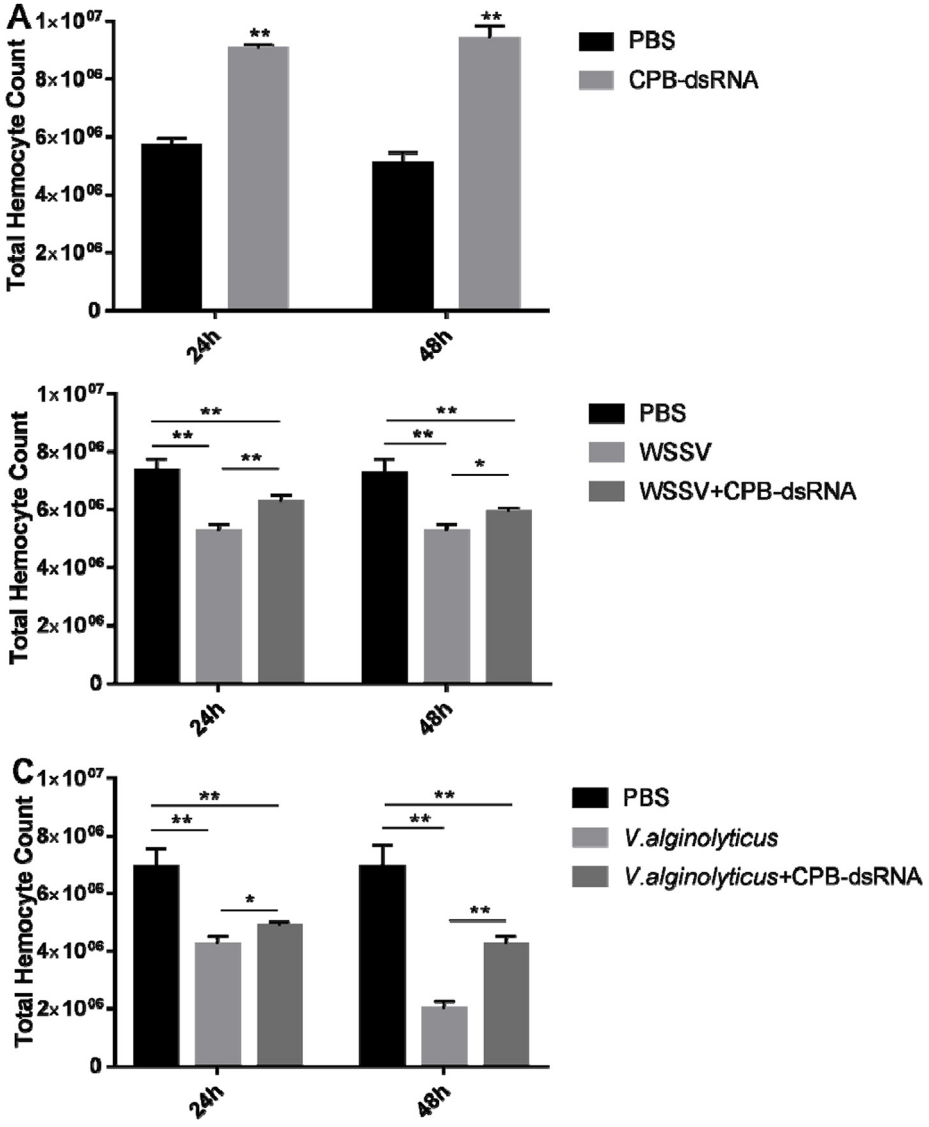

Fig. 10. Influence of *carboxypeptidase B-like* knockdown on total hemocyte count. (A) THC of the crabs treated with *carboxypeptidase B-like* dsRNA (CPB-dsRNA). (B) THC of WSSV challenged crabs treated with CPB-dsRNA. (C) THC of *V. alginolyticus* challenged crabs treated with CPB-dsRNA. Data are expressed as percentage of control. Indicates values significantly different (**$p < 0.01$) from the control.

groups, and the copy number was always lower in the CPB-dsRNA-treated group compared with the respective control (Fig. 8). Copy numbers increased to 10^5 and 10^6, respectively, at 72 h post-infection. Compared with the control groups, crabs in the experimental groups had lower copy numbers of virions, suggesting that the RNAi of CPB led to a remarkable suppression of WSSV replication, indicating that CPB may promote the replication of WSSV.

We evaluated the effects of the CPB gene on the mortality of pathogen-challenged crabs by injecting them with CPB-dsRNA and then challenging them with WSSV or *V. alginolyticus*. WSSV infected crabs treated with CPB-dsRNA had significantly higher survival at 12, 24, 36, 60, and 72 h post-challenge, compared with crabs challenged with WSSV alone (Fig. 9A). The negative control showed a cumulative mortality of zero (Fig. 9A), indicating that CPB-dsRNA itself was non-toxic in crabs. However, CPB-dsRNA had a different effect on mortality in *V. alginolyticus*-infected crabs. The cumulative mortality following CPB-dsRNA + *V. alginolyticus* treatment was significantly higher than that following *V. alginolyticus* alone ($p < 0.01$), starting from 12 h post-challenge (Fig. 9B). Overall, these results indicated that CPB was vital for WSSV infection, while, in contrast, the absence of CPB increased crab mortality following *V. alginolyticus* infection.

3.8. Influence of carboxypeptidase B-like knockdown on total hemocyte count

Treatment with CPB-dsRNA significantly increased ($p < 0.01$) the total hemocyte counts (THC) compared with phosphate-buffered saline (PBS)-treated controls at 24 and 48 h post-treatment (Fig. 10A). The THC was significantly reduced at ($p < 0.01$) 24 and 48 h after WSSV treatment, compared with PBS controls. The THC of CPB-dsRNA + WSSV was significantly decreased compared with the PBS group at 24 and 48 h. However, the THC of CPB-dsRNA + WSSV was significantly higher than in the WSSV alone group (Fig. 10B). Similarly, the THC was significantly decreased at 24 and 48 h after *V. alginolyticus* and CPB-dsRNA + *V. alginolyticus* treatment, compared with the PBS control. However, the THC of CPB-dsRNA + *V. alginolyticus* was significantly higher than in the *V. alginolyticus* alone group (Fig. 10C). These results suggest that CPB may negatively regulate hemocyte proliferation in crabs.

3.9. Effect of carboxypeptidase B-like on phagocytosis

To characterize the role of CPB in phagocytosis, the expression of

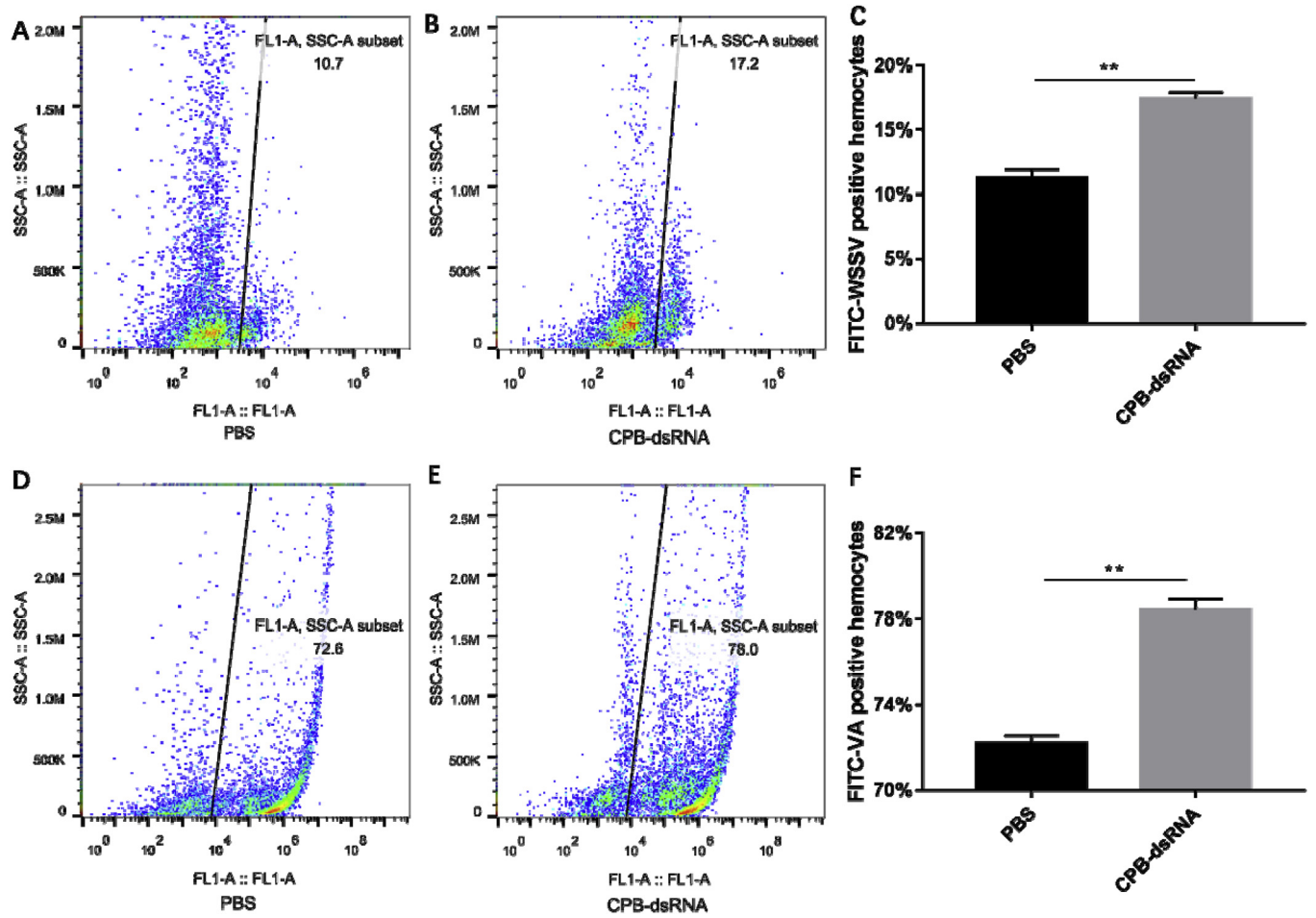

Fig. 11. Flow cytometry assay of phagocytosis by crab hemocyte. Inactivated WSSV and *V. alginolyticus* particles were labeled with FITC. (A) PBS; (B) CPB-dsRNA; (C) bar graph of phagocytosis of WSSV; (D) PBS; (E) CPB-dsRNA; (F) bar graph of phagocytosis of *V. alginolyticus*. The significant differences between treatments are indicated with asterisks (**$p < 0.01$).

CPB was knocked down and then the phagocytic activity of crab hemocytes was assessed. When CPB was silenced, the crab phagocytic activity against WSSV was dramatically strengthened compared with controls (Fig. 11C). Similarly, when CPB was silenced, the crab phagocytic activity against *V. alginolyticus* was dramatically strengthened compared with controls (Fig. 11F). The number of WSSV copies indicates that CPB may exert negative effects on antiviral phagocytosis in crabs.

3.10. Effect of carboxypeptidase B-like on apoptosis

We investigated the role of CPB in the apoptosis of crab hemocytes using an Annexin V-FITC Apoptosis Detection Kit I (BD Biosciences, USA). The apoptosis rate was lower in the WSSV group compared with the CPB-dsRNA-treated group (41.7% vs. 65.3%) (Fig. 12). Similarly, the apoptosis rate was significantly increased in the group of crabs first treated with CPB-dsRNA, then infected with *V. alginolyticus*, compared to crabs infected with *V. alginolyticus* (Fig. 12). These results suggested that the CPB had an inhibitory effect on hemocyte apoptosis in crabs infected with WSSV or *V. alginolyticus*.

4. Discussion

CPB was first isolated from the porcine pancreas and was later found to be expressed in different tissues of several animals with different potential functions [33,34]. In the human brain, CPB is expressed and secreted by endoplasmic reticulum cells of brain neurons [35]. Plasma CPB is produced by the liver and circulates in the blood. It is activated by thrombin and functions in the inhibition of fibrinolysis, and its expression level is associated with a range of diseases [21,36]. An increase in the concentration of plasma CPB in the blood increases the concentration of cholesterol and fibrinogen and is one of the causative factors of coronary heart disease. The CPB precursor is very stable and does not bind to other substances in urine. The determination of CPB precursor concentration in urine is an effective method for accurately predicting the severity of acute pancreatitis [37]. The concentration of bradykinin is inversely related to the activity of plasma CPB. Therefore, it is considered that the decrease in plasma CPB activity leads to an increase in the concentration of bradykinin, which causes a decrease in blood pressure and shock [38]. CPB has also been shown to cleave and inactivate several inflammatory proteins, namely C5a, C3a, bradykinin, and thrombin-cut osteopontin [39]. Its ability to modulate inflammatory substrates suggests that CPB may also act to inhibit inflammation. Consistent with this concept, we previously found that CPB prevents rheumatoid arthritis by inhibiting C5a-mediated inflammation in the synovial joint [40]. Previous studies have demonstrated that CPB is closely related to human diseases, and in recent years, the acquisition of invertebrate CPB gene clones, such as *Hyalella Azteca*, *Mizuhopecten yessoensis*, and *Drosophila willistoni*, form the basis of studying CPB gene sequences in invertebrates [41,42].

The whole coding sequence, denoted as CPB, comprises 2316 nucleotides and 434 amino acid residues. Neighbor-joining tree analysis revealed a close evolutionary relationship with the CPB protein in *Hyalella Azteca*. Furthermore, the protein was expressed at varying

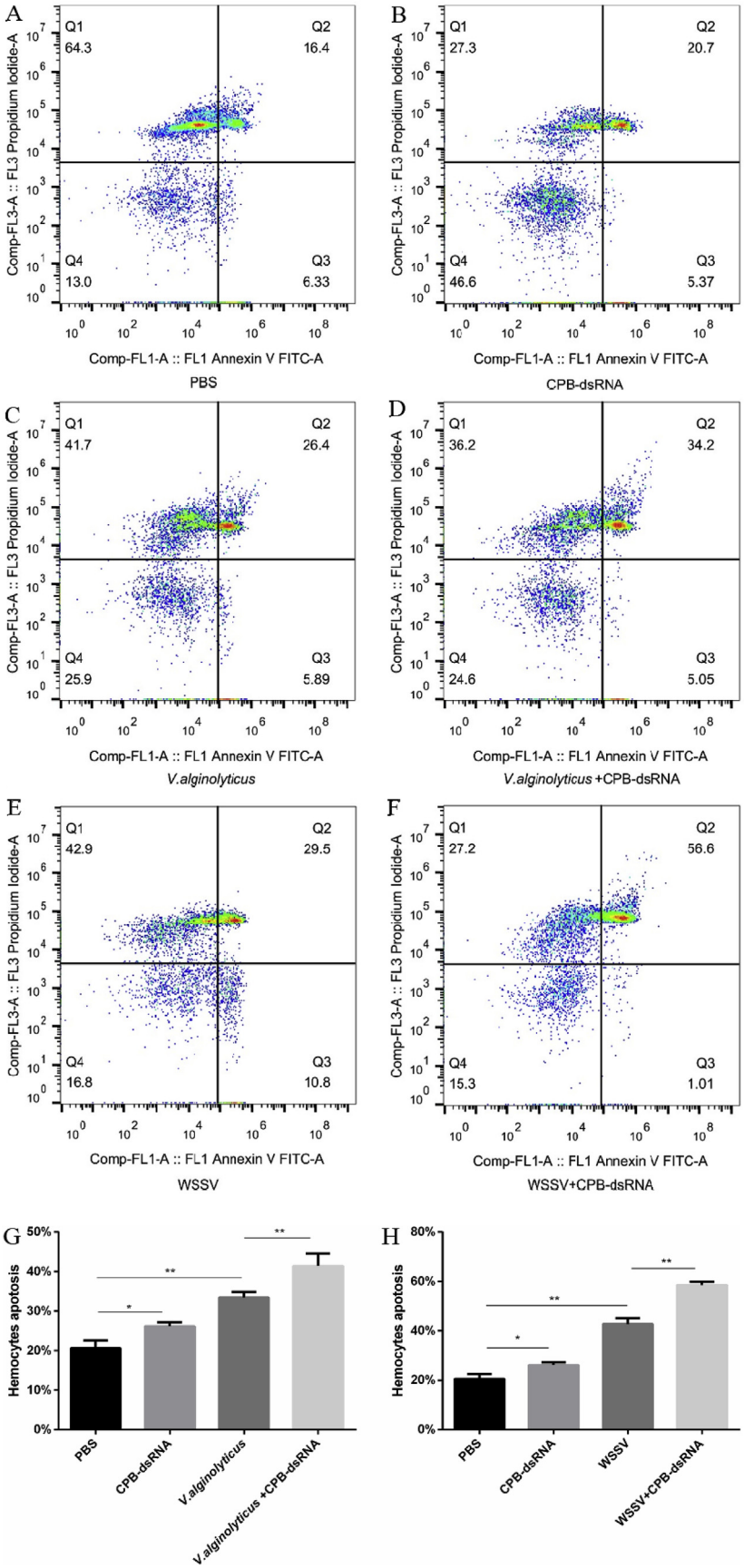

Fig. 12. Flow cytometry assay of hemocyte apoptosis. (A) PBS; (B) CPB-dsRNA; (C) *V. alginolyticus*; (D) *V. alginolyticus* + CPB-dsRNA; (E) WSSV; (F) WSSV + CPB-dsRNA; (G) Bar graph of phagocytosis of *V. alginolyticus*; (H) Bar graph of phagocytosis of WSSV. Double asterisks indicate a significant difference ($P < 0.01$) between the sample and the challenge only.

levels in all the examined tissues from *S. paramamosain*, with the highest levels in hepatopancreas and relatively low levels in the hemolymph, gills, intestines, heart, and muscles. In contrast, previous reports have detected the highest expression levels in the intestines of insects [43,44]. The expression of CPB was high in the hepatopancreas, which is an important immune organ in crustaceans, but CPB expression was significantly decreased by challenge with WSSV or *V. alginolyticus*. However, compared with the low expression levels of CPB in *V. alginolyticus*-challenged crabs from 12 to 48 h post-infection, expression levels returned to those of the control at 48 h post-infection with WSSV. The decrease of CPB expression following WSSV or *V. alginolyticus* infection indicates CPB may anticipate the innate immune response of crabs. Combining with the high phagocytosis rate of *V. alginolyticus* by hemocytes when CPB wan knocked down, indicating that CPB may regulate hemocyte phagocytosis when *V. alginolyticus* infection in crabs.

RNAi is a phenomenon of post-transcriptional gene silencing specifically mediated by dsRNA sequences in vivo [45]. RNAi has previously been used to reveal the functions of some proteins in shrimp immunity [46] and has been widely applied in studies of the immune response in many invertebrate models to investigate the antibacterial and antiviral mechanisms of certain target proteins [47]. In this study, we examined the role of *S. paramamosain* CPB in innate immunity by inhibiting its expression using CPB-dsRNA. We also determined the effects of CPB-dsRNA on the expression levels of several typical innate immune molecules and signal transduction factors. The knockdown of CPB mRNA led to significant down-regulation of the innate immune factors *JAK*, *STAT*, *C-type-lectin*, *CAP*, *TLRs*, *proPO*, and *myosin*. TLRs are a class of proteins that play a key role in the innate immune system. The Toll pathway in invertebrates, such as *Drosophila melanogaster*, is activated by different stimuli, including Gram-positive bacteria, fungi and virulence factors [48,49]. Members of the signal transducer and activator of transcription (STAT) protein family are intracellular transcription factors that mediate many aspects of cellular immunity, proliferation, apoptosis, and differentiation. Gene knockout studies have provided evidence that STAT proteins are involved in the development and function of the immune system and play a role in maintaining immune tolerance and tumor surveillance [50]. Proteins containing a C-type lectin domain have multiple functions including cell–cell adhesion, the immune response to pathogens, and apoptosis [51,52]. The results suggest that the CPB impacts on the processes of apoptosis and phagocytosis. Apoptosis is a highly regulated programmed cell death process and plays a critical role in virus infection. The host may promote apoptosis so as to enhance resistance to virus infection [53]. Osteopontin (OPN) is known to be a pro-inflammatory cytokine that plays an important role in the pathogenesis of rheumatoid arthritis. OPN has anti-apoptotic effects on different cell types [54–56]. Consistent with this, OPN inhibits neutrophil apoptosis, and CPB could indirectly regulate the process of apoptosis [57]. It was reported that thrombin-activated CPB plays a central homeostasis role in rheumatoid arthritis by regulating neutrophil viability and reducing synovial cell adhesion [57]. In our study, apoptosis was increased in CPB-dsRNA-treated crabs challenged with WSSV or *V. alginolyticus*, indicating that the CPB may regulate apoptosis of host hemocytes and suppress apoptosis during WSSV or *V. alginolyticus* infection. Studies have shown that phagocytosis is required for host antiviral immunity through the direct rapid engulfment of virions and apoptotic cells [58–60]. Our phagocytosis results indicated that the CPB may regulate phagocytosis and exert negative effects on phagocytosis in crabs.

However, the lower number of WSSV copies and mortality in the CPB knockdown group suggested that WSSV could utilize CPB to promote its own replication. According to our observation in this study, fewer hemocytes were obtained from virus-infected crabs compared with healthy crabs, and the same was seen in bacteria-infected individuals. Hemocyte is very important in the innate immunity of crustaceans and it is involved in cellular immunity and humoral immunity, and it can directly recognize and engulf foreign pathogens [61]. Compared to the group infected only with the virus or vibrio, the total hemocytes were increased in WSSV or *V. alginolyticus* infection crabs when pretreated with CPB-dsRNA. Furthermore, immune parameters such as SOD activity, as well as THC, were promoted by the absence of CPB in crabs. SOD activity is important indicator for identifying the immunological activity of crustaceans [62–65].

The results suggested that crab CPB may play a positive role in the immune response to *V. alginolyticus* through increasing the phagocytosis rate of *V. alginolyticus*. The CPB showed important immune function in crabs, whereas WSSV could take advantage of the CPB to promote viral replication through inhibiting the host cell apoptosis. These new findings provide an important basis for further exploration of the innate immune mechanism of marine crabs.

Acknowledgments

This work was financially supported by National Key Research and Development Program of China (2018YFD0500300) and Qianjiang talent program (QJD1602023).

References

[1] Z. Lin, M. Hao, Y. Huang, W. Zou, H. Rong, X. Wen, Cloning, tissue distribution and nutritional regulation of a fatty acyl Elovl 4-like elongase in mud crab, *Scylla paramamosain* (Estampador, 1949), Comp. Biochem. Physiol. B 217 (2018) 70–78.
[3] Z. Wang, B. Sun, F. Zhu, The shrimp hormone receptor acts as an anti-apoptosis and anti-inflammatory factor in innate immunity, Fish Shellfish Immunol. 72 (2018) 581–583.
[4] V.N. Ut, L.L. Vay, T.T. Nghia, T.T.H. Hanh, Development of nursery culture techniques for the mud crab *Scylla paramamosain* (Estampador), Aquacult. Res. 38 (2007) 1563–1568.
[5] W. Wang, Bacterial diseases of crabs: a review, J. Invertebr. Pathol. 106 (2011) 0–26.
[6] B. Sun, Z. Wang, Z. Wang, X. Ma, F. Zhu, A proteomic study of hemocyte proteins from mud crab (*Scylla paramamosain*) infected with white spot syndrome virus or *Vibrio alginolyticus*, Front. Immunol. 8 (2018) 468.
[7] D. Galván-Alvarez, F. Mendoza-Cano, J. Hernández-López, A. Sánchez-Paz, Experimental evidence of metabolic disturbance in the white shrimp *Penaeus vannamei* induced by the Infectious Hypodermal and Hematopoietic Necrosis Virus (IHHNV), J. Invertebr. Pathol. 111 (2010) 60–67.
[8] D.L. Diamond, A.J. Syder, J.M. Jacobs, C.M. Sorensen, K.A. Walters, S.C. Proll, et al., Temporal proteome and lipidome profiles reveal hepatitis C virus-associated reprogramming of hepatocellular metabolism and bioenergetics, PLoS Pathog. 6 (2010) e1000719.
[9] J. Munger, S.U. Bajad, H.A. Coller, T. Shenk, J.D. Rabinowitz, Dynamics of the cellular metabolome during human cytomegalovirus infection, PLoS Pathog. 2 (2006) e132.
[10] J. Munger, B.D. Bennett, A. Parikh, X.J. Feng, J. McArdle, H.A. Rabitz, et al., Systems-level metabolic flux profiling identifies fatty acid synthesis as a target for antiviral therapy, Nat. Biotechnol. 26 (2008) 1179–1186.
[11] I.T. Chen, T. Aoki, Y.T. Huang, I. Hirono, T.C. Chen, J.Y. Huang, et al., White spot syndrome virus induces metabolic changes resembling the warburg effect in shrimp hemocytes in the early stage of infection, J. Virol. 85 (2011) 12919–12928.
[12] Y.Y. Li, X.A. Xia, Q.Y. Wu, W.H. Liu, Y.S. Lin, Infection with *Hematodinium* sp. in mud crabs *Scylla serrata* cultured in low salinity water in southern China, Dis. Aquat. Org. 82 (2008) 145–150.
[13] J.G. Chen, D. Lou, J.F. Yang, Isolation and identification of *Acholeplasma* sp. from the mud crab, *Scylla serrata*, evid based compl, Altern. Med. 2011 (2011) 1–5.
[14] S. Li, L. Sun, H. Wu, Z. Hu, W. Liu, Y. Li, et al., The intestinal microbial diversity in mud crab (*Scylla paramamosain*) as determined by PCR-DGGE and clone library analysis, J. Appl. Microbiol. 113 (2012) 1341–1351.
[15] M. Danta, N. Semmo, P. Fabris, D. Brown, O.G. Pybus, C.A. Sabin, et al., Impact of HIV on host-virus interactions during early hepatitis C virus infection, J. Infect. Dis. 197 (2008) 1558–1566.
[16] M. Garand, J.H. Lin, B. Zagorac, M.L. Koschinsky, M.B. Boffa, Regulation of the gene encoding human thrombin-activatable fibrinolysis inhibitor by estrogen and progesterone, Blood Coagul. Fibrinolysis 24 (2013) 393–404.
[17] D. Wang, H. Fang, H. Chen, H. Chen Carboxypeptidase, A/B subfamily, Chin. J. Biochem. Pharm. 26 (2005) 55–58.
[18] A.J. Barrett, N.D. Rraw lings, J.F. Woessner, Handbook of Proteolytic Enzymes, Academic Press, San Diego, 1998, pp. 1318–1335.
[19] G.R. Folkart, J. Dancis, W.L. Money, Transfer of carbohydrates across Guinea pig placenta, Am. J. Obstet. Gynecol. 80 (1960) 221–223.
[20] M.B. Boffa, T.S. Reid, E. Joo, M.E. Nesheim, M.L. Koschinsky, Characterization of the gene encoding human TAFI (thrombin-activable fibrinolysis inhibitor; plasma procarboxypeptidase B), Biochemistry 38 (1999) 6547–6558.
[21] B.N. Bouma, J.C. Meijers, Thrombin-activatable fibrinolysis inhibitor (TAFI, plasma procarboxypeptidase B, procarboxypeptidase R, procarboxypeptidase U), J. Thromb. Haemost. 1 (2003) 1566–1574.

[22] H. Papp, I. Török, A. Matsumoto, T. Enomoto, S. Matsuyama, P. Kása, Expression and distribution of carboxypeptidase B in the hippocampal subregions of normal and Alzheimer's disease brain, Acta Biol. Hung. 54 (2003) 55–62.
[23] M. Edge, C. Forder, J. Hennam, I. Lee, D. Tonge, I. Hardern, et al., Engineered human carboxypeptidase B enzymes that hydrolyse hippuryl-L-glutamic acid: reversed-polarity mutants, Protein Eng. 11 (1998) 1229–1234.
[24] R. Pezzilli, A.M. Morselli-Labate, A.R. Barbieri, L. Platè, Clinical usefulness of the serum carboxypeptidase B activation peptide in acute pancreatitis, JOP 1 (2000) 58–68.
[25] F. Zhu, X. Zhang, Protection of shrimp against white spot syndrome virus (WSSV) with β-1,3-D-glucan-encapsulated vp28-siRNA particles, Mar. Biotechnol. 14 (2012) 63–68.
[26] M. Huang, Y. Liu, C. Xie, W.N. Wang, LvDJ-1 plays an important role in resistance against *Vibrio alginolyticus* in *Litopenaeus vannamei*, Fish Shellfish Immunol. 44 (2015) 180–186.
[27] K.J. Livak, T.D. Schmittgen, Analysis of relative gene expression data using real-time quantitative PCR and the 2(-Delta Delta C(T)) Method, Methods 25 (2011) 402–408.
[28] W. Liu, F. Han, X. Zhang, Ran GTPase regulates hemocytic phagocytosis of shrimp by interaction with myosin, J. Proteome Res. 8 (2009) 1198–1206.
[29] F. Zhu, X. Zhang, The Wnt signaling pathway is involved in the regulation of phagocytosis of virus in *Drosophila*, Sci. Rep. 3 (2013) 1–9.
[30] K. Wongprasert, T. Rudtanatip, J. Praiboon, Immunostimulatory activity of sulfated galactans isolated from the red seaweed *Gracilaria fisheri* and development of resistance against white spot syndrome virus (WSSV) in shrimp, Fish Shellfish Immunol. 36 (2014) 52–60.
[31] Z. Zhao, C. Jiang, X. Zhang, Effects of immunostimulants targeting Ran GTPase on phagocytosis against virus infection in shrimp, Fish Shellfish Immunol. 31 (2011) 1013–1018.
[32] C.O. Beauchamp, I. Fridovich, Isozymes of superoxide dismutase from wheat germ, Biochim. Biophys. Acta 317 (1973) 50–64.
[33] V. Villegas, J. Vendrell, X. Avilés, The activation pathway of procarboxypeptidase B from porcine pancreas: participation of the active enzyme in the proteolytic processing, Protein Sci. 4 (1995) 1792–1800.
[34] A.N. Vernigora, N.V. Shchetinina, D.A. Saldaev, M.T. Gengin, Distribution of activities of alkaline carboxypeptidases in tissues of laboratory animals of different species, J. Evol. Biochem. Physiol. 38 (2002) 31–34.
[35] A. Matsumoto, K. Itoh, T. Seki, K. Motozaki, S. Matsuyama, Human brain carboxypeptidase B, which cleaves β-amyloid peptides *in vitro*, is expressed in the endoplasmic reticulum of neurons, Eur. J. Neurosci. 13 (2001) 1653–1657.
[36] X.Y. Du, B.A. Zabel, T. Myles, S.J. Allen, T.M. Handel, P.P. Lee, et al., Regulation of chemerin bioactivity by plasma carboxypeptidase N, carboxypeptidase B (activated thrombin-activable fibrinolysis inhibitor), and platelets, J. Biol. Chem. 284 (2009) 751–758.
[37] S. Tani, H. Akatsu, Y. Ishikawa, N. Okada, H. Okada, Preferential detection of procarboxypeptidase R by enzyme-linked immunosorbent assay, Microbiol. Immunol. 47 (2003) 295–300.
[38] Y. Tsuboi, M. Takahashi, Y. Ishikawa, H. Okada, T. Yamada, Elevated bradykinin and decreased carboxypeptidase R as a cause of hypotension during tryptophan column immunoabsorption therapy, Ther. Apher. 2 (1998) 297–299.
[39] L.L. Leung, T. Myles, T. Nishimura, J.J. Song, W.H. Robinson, Regulation of tissue inflammation by thrombin-activatable carboxypeptidase B (or TAFI), Mol. Immunol. 45 (2008) 4080–4083.
[40] J.J. Song, I. Hwang, K.H. Cho, M.A. Garcia, A.J. Kim, T.H. Wang, et al., Plasma carboxypeptidase B downregulates inflammatory responses in autoimmune arthritis, J. Clin. Investig. 121 (2011) 3517–3527.
[41] D.P. Weston, H.C. Poynton, G.A. Wellborn, M.J. Lydy, B.J. Blalock, M.S. Sepulveda, et al., Multiple origins of pyrethroid insecticide resistance across the species complex of a nontarget aquatic crustacean, *Hyalella azteca*, Proc. Natl. Acad. Sci. U.S.A. 110 (2013) 16532–16537.
[42] Drosophila 12 Genomes Consortium, A.G. Clark, M.B. Eisen, D.R. Smith, C.M. Bergman, B. Oliver, et al., Evolution of genes and genomes on the *Drosophila* phylogeny, Nature 450 (2007) 203–218.
[43] J. Xiu, C. Wei, X. Shang, G. Guo, Q. Wu, J. Wu, Cloning and prokaryotic expression of *Musca domestica* carboxypeptidase gene, Guangdong Agric. Sci. 10 (2014) 152–154.
[44] X. Xin, R. Day, W. Dong, Y. Lei, L.D. Fricker, Cloning, sequence analysis, and distribution of rat metallocarboxypeptidase Z, DNA Cell Biol. 17 (1998) 311–319.
[45] A. Fire, S. Xu, M.K. Montgomery, S.A. Kostas, S.E. Driver, C.C. Mello, Potent and specific genetic interference by double-stranded RNA in *Caenorhabditis elegans*, Nature 391 (1998) 806–811.
[46] J. Robalino, C.L. Browdy, S. Prior, A. Metz, P. Parnell, P. Gross, et al., Induction of antiviral immunity by double-stranded RNA in a marine invertebrate, J. Virol. 78 (2004) 10442–10448.
[47] G.J. Hannon, RNA interference, Nature 418 (2002) 244–451.
[48] D. Ferrandon, J.L. Imler, C. Hetru, J.A. Hoffmann, The *Drosophila* systemic immune response: sensing and signalling during bacterial and fungal infections, Nat. Rev. Immunol. 7 (2007) 862–874.
[49] R.S. Mahla, M.C. Reddy, D.V. Prasad, H. Kumar, Sweeten, PAMPs: role of sugar complexed PAMPs in innate immunity and vaccine biology, Front. Immunol. 4 (2013) 1–16.
[50] U. Vinkemeier, I. Moarefi, J.E. Darnell, J. Kuriyan, Structure of the amino-terminal protein interaction domain of STAT-4, Science 279 (1998) 1048–1052.
[51] K. Drickamer, C-type lectin-like domains, Curr. Opin. Struct. Biol. 9 (1999) 585–590.
[52] A. Cambi, C. Figdor, Necrosis: C-type lectins sense cell death, Curr. Biol. 19 (2009) 375–378.
[53] A. Roulston, R.C. Marcellus, P.E. Branton, Viruses and apoptosis, Annu. Rev. Microbiol. 53 (1999) 577–628.
[54] T.H. Burdo, M.R. Wood, H.S. Fox, Osteopontin prevents monocyte recirculation and apoptosis, J. Leukoc. Biol. 81 (2007) 1504–1511.
[55] M. Scatena, M. Almeida, M.L. Chaisson, N. Fausto, R.F. Nicosia, C.M. Giachelli, NF-κB mediates αvβ3 integrin-induced endothelial cell survival, J. Cell Biol. 141 (1998) 1083–1093.
[56] Y.H. Lin, H.F. Yang-Yen, The osteopontin-CD44 survival signal involves activation of the phosphatidylinositol 3-kinase/Akt signaling pathway, J. Biol. Chem. 276 (2001) 46024–46030.
[57] S.A. Sharif, X. Du, T. Myles, J.J. Song, E. Price, D.M. Lee, et al., Thrombin-activatable carboxypeptidase B cleavage of osteopontin regulates neutrophil survival and synoviocyte binding in rheumatoid arthritis, Arthritis Rheum. 60 (2009) 2902–2912.
[58] Y. Hashimoto, T. Moki, T. Takizawa, A. Shiratsuchi, Y. Nakanishi, Evidence for phagocytosis of influenza virus-infected, apoptotic cells by neutrophils and macrophages in mice, J. Immunol. 178 (2007) 2448–2457.
[59] K.M. Chung, B.S. Thompson, D.H. Fremont, M.S. Diamond, Antibody recognition of cell surface-associated NS1 triggers Fc-gamma receptor-mediated phagocytosis and clearance of West Nile Virus-infected cells, J. Virol. 81 (2007) 9551–9555.
[60] T. Ye, W. Tang, X. Zhang, Involvement of Rab6 in the regulation of phagocytosis against virus infection in invertebrates, J. Proteome Res. 11 (2012) 4834–4846.
[61] R. Bettencourt, H. Asha, C. Dearolf, Y.T. Ip, Hemolymph-dependent and -independent responses in *Drosophila* immune tissue, J. Cell. Biochem. 92 (2004) 849–863.
[62] K. Sritunyalucksana, K. Soderhall, The ProPO and clotting system in Crustaceans, Aquaculture 191 (2000) 53–69.
[63] A. Tassanakajon, K. Somboonwiwat, P. Supungul, S. Tang, Discovery of immune molecules and their crucial functions in shrimp immunity, Fish Shellfish Immunol. 34 (2013) 954–967.
[64] P.T. Schumacker, Reactive oxygen species in cancer: a dance with the devil, Cancer Cell 27 (2015) 156–157.
[65] A.I. Campa-Córdova, N.Y. Hernández-Saavedra, R. De Philippis, F. Ascencio, Generation of superoxide anion and SOD activity in haemocytes and muscle of American white shrimp (*Litopenaeus vannamei*) as a response to beta-glucan and sulphated polysaccharide, Fish Shellfish Immunol. 12 (2002) 353–366.

浙江农林大学图书馆收录证明报告

《SCI-Expanded》检索结果（收录情况）

WEB OF SCIENCE™

Web of Science™ Core Collection

经检索《Web of Science™ Core Collection》，朱斐 发表的下述 1 篇论文被《SCI-Expanded》收录。（检索时间：2019 年 12 月 13 日）

第 1 条，共 1 条

标题: Molecular characterization of carboxypeptidase B-like (CPB) in Scylla paramcunosain a nd its role in white spot syndrome virus and Vibrio alginolyticus infection

作者: Qian, XY (Qian, Xiyi); Lai, YY (Lai, Yongyong); Zhu, F (Zhu, Fei)

来源出版物: FISH & SHELLFISH IMMUNOLOGY 卷: 94 页: 434-446 **DOI:** 10.1016/j.fsi.2019.09.036 出版年: NOV 2019

Web of Science 核心合集中的 "被引频次": 0

被引频次合计: 0

入藏号: WOS:000496892400047

PubMed ID: 31536767

地址: [Qian, Xiyi; Lai, Yongyong; Zhu, Fei] Zhejiang Agr & Forestry Univ, Coll Anim Sci & T echnol, Zhejiang Prov Engn Lab Anim Hlth Inspect & Intern, Hangzhou 311300, Zhejiang, Peoples R China.

通讯作者地址: Zhu, F (通讯作者), Zhejiang Agr & Forestry Univ, Coll Anim Sci & Technol, Zhejiang Prov Engn Lab Anim Hlth Inspect & Intern, Hangzhou 311300, Zhejiang, Peoples R China.

电子邮件地址: zhufei@zju.edu.cn

ISSN: 1050-4648

eISSN: 1095-9947

注：以上检索结果均得到被检索人的确认。

《SCI-Expanded》检索结果（收录情况）

浙江农林大学图书馆

检索人：桑宇芳

2019 年 12 月 13 日